

Porous waveguide facilitated low divergence quantum cascade laser*

Yin Wen(尹雯), Lu Quanyong(陆全勇), Liu Wanfeng(刘万峰), Zhang Jinchuan(张锦川), Wang Lijun(王利军), Liu Junqi(刘俊岐), Li Lu(李路), Liu Fengqi(刘峰奇)[†], and Wang Zhanguo(王占国)

Key Laboratory of Semiconductor Materials Science, Institute of Semiconductors, Chinese Academy of Sciences, Beijing 100083, China

Abstract: A quantum cascade laser with a porous waveguide structure emitting at $4.5\ \mu\text{m}$ is reported. A branch-like porous structure filled with metal material was fabricated on both sides of the laser ridge by an electrochemical etching process. In contrast to the common ridge waveguide laser, devices with a porous structure give rather better beam quality. Utilizing this porous structure as a high-order mode absorber, the device exhibited fundamental transverse mode emission with a nearly diffraction limited far-field beam divergence angle of 4.9° .

Key words: quantum cascade laser; ridge waveguide; porous structure; electrochemical etching

DOI: 10.1088/1674-4926/32/6/064008

PACC: 4255P; 7850G

1. Introduction

The quantum cascade laser (QCL) is one of the most promising light sources for mid- and infrared ranges for trace gas analysis, space communication and other applications^[1–3]. A highly efficient laser beam with small divergence angle should be ideal for these applications. However, the common ridge structure devices usually suffer from poor far-field characteristics because the relatively wide ridge is prone to high-order transverse mode operation. Some ordinary methods to achieve fundamental transverse mode emitting and a small far-field divergence angle like angled-grating and photonic crystal has always resulted in a complicated and costly fabrication procedure^[4–6]. Theoretical and experimental results have proved that high-order transverse mode can be effectively eliminated by adding side absorbers to the upper waveguide in terahertz QCLs^[7]. Inspired by the above results, we explored the feasibility of using porous InP filled with metal on both sides of a waveguide to absorb the optical feedback of high-order transverse modes.

Electrochemical etching is a microfabrication technology for III–V semiconductor materials that can provide a microporous array structure, at very low cost and using simple equipment^[8]. In this paper, we present a new pattern ridge waveguide QCL with porous side absorbers formed by electrochemical etching. A laser with side absorbers emitted at fundamental transverse mode with a beam divergence angle of only 4.9° .

2. Device design and fabrication procedure

The QCL wafer was grown on an n-doped (Si, $2 \times 10^{17}\ \text{cm}^{-3}$) InP substrate by solid-source molecular beam epitaxy in a single growth step. The active region consists of 30

stages designed to emit at $4.5\ \mu\text{m}$, similar to Ref. [9]. The upper cladding layer consists of a $2.4\text{-}\mu\text{m}$ -thick n-InP (Si, $2.2 \times 10^{16}\ \text{cm}^{-3}$), followed by a 500-nm-thick n-InP cap layer with graded doping (Si, 2.5×10^{18} – $1.0 \times 10^{19}\ \text{cm}^{-3}$).

The fabrication of the porous structure was based on electrochemical etching of semiconductor material using a simple three-electrode cell. It involved a Pt counter electrode, a reference saturated calomel electrode (SCE), and a QCL wafer electrode whose cap layer surface was dipped into the acid electrolyte. The electrolyte was a HCl-based aqueous solution containing HNO_3 (200 mL of 1 mol/L HCl + 3 mL of HNO_3). A constant bias of 5 V was applied by a potentiostat and the whole etching time was 300 ms, under dark conditions at 5°C .

The wafer was processed by conventional photolithogra-

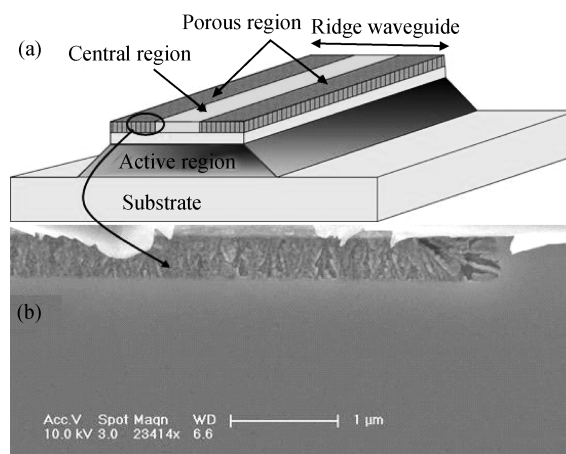


Fig. 1. (a) Schematic diagram of a double-channel ridge waveguide structure with double-sided porous regions. (b) Scanning electron microscope image of the porous region in the cap InP layer.

* Project supported by the National Science Fund for Distinguished Young Scholars and other Research Projects of China (Nos. 60525406, 60736031, 60806018, 60906026, 2006CB604903, 2007AA03Z446, 2009AA03Z403).

[†] Corresponding author. Email: fqliu@semi.ac.cn

Received 22 November 2010, revised manuscript received 20 December 2010

© 2011 Chinese Institute of Electronics

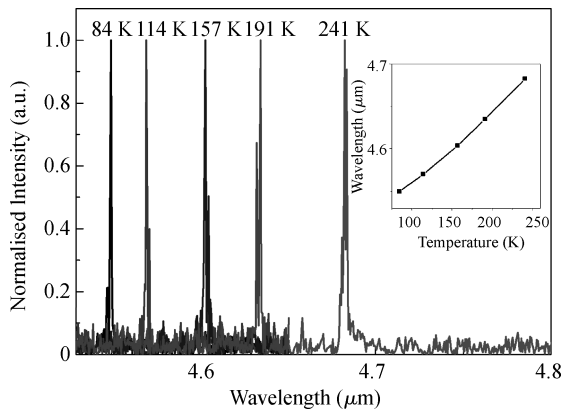


Fig. 2. Lasing spectra (2 μ s, 5 kHz, duty cycle of 1%) of a 48- μ m-wide RWG device with a porous region at different temperatures. The inset shows the linear tuning characteristics of the wavelength with temperature.

phy and wet chemical etching in a $\text{HNO}_3 : \text{HBr} : \text{H}_2\text{O}$ (1 : 1 : 10) solution to form a double-channel structure with a 2-mm-long, overall 48- μ m-wide ridge waveguide (RWG) containing porous region and central region, as shown in Fig. 1(a). The width of the central region without the porous structure was about 5.5 μ m. The whole ridge was etched down to the InP substrate to form a strong index guided waveguide. A 350-nm-thick SiO_2 layer served as an electrical insulation layer and Ti-Au was used as the top contact metal. Thinning, back contacting (Ge-Au-Ni-Au) and cleaving completed processing. For comparison, a 2-mm-long and 48- μ m-wide ridge QCL without a porous region was fabricated from the same wafer. For characterization, all devices were mounted ridge side up on copper heatsinks with indium solder.

3. Results

A branch-like porous structure, shown in Fig. 1(b), was fabricated in the cap layer of the QCL by electrochemical etching and the direction of the holes was basically along the orientation of the electrical field. For characterization, the devices were placed on a temperature-controlled cold finger in an evacuated liquid nitrogen cryostat. The spectral measurements were carried out using a Fourier transform infrared (FTIR) spectrometer in step scan mode with a resolution of 1 cm^{-1} . Current pulses of 2 μ s duration with a 5 kHz repetition frequency were applied to the device. The emission spectra measured at different temperatures are shown in Fig. 2. The inset of the figure shows that the emission wavelengths red shift with temperature and the data can be fitted by a linear function. The wavelength is tuned from 4.550 μ m at 84 K to 4.683 μ m at 241 K with a wavelength-temperature tuning coefficient of $\Delta\lambda/\Delta T \approx 0.85 \text{ nm/K}$.

The horizontal far-field distribution was measured with a liquid nitrogen-cooled HgCdTe detector at a distance of 10 cm without any focus element. Figure 3 illustrates the measured horizontal beam divergence for both the general RWG QCL and the QCL with a porous region at 80 K under a pulsed injection current (2 μ s & 5 kHz) of 600 mA. The RWG QCL displays a high-order mixed mode emission with a divergence

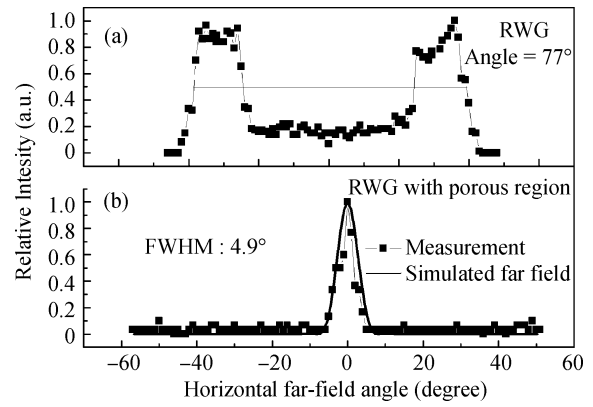


Fig. 3. Horizontal far-field pattern of a normal RWG QCL and an RWG QCL with a porous region. (a) Measured far-field pattern for a 48- μ m-wide ridge RWG QCL. (b) Measured single-lobe far-field pattern for a RWG QCL with a porous side absorber and the corresponding simulated result.

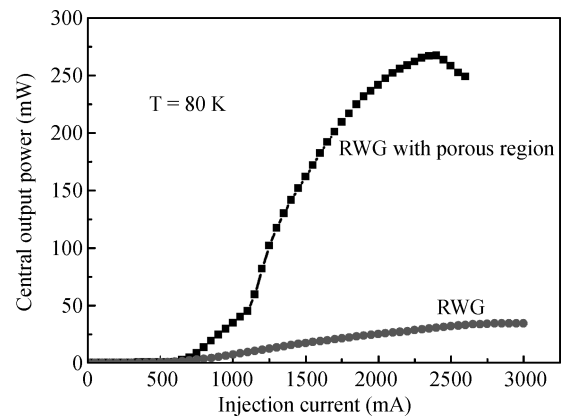


Fig. 4. Central light output characteristic of a normal RWG QCL and a RWG QCL with a porous region at 80 K. A driving current with 2- μ s-width and 5-kHz-repetition was used in the measurement.

angle of about 77°. However, a QCL with a porous region exhibits only a single-lobe far-field pattern with a divergence angle of $\text{FWHM} \approx 4.9^\circ$. Compared with that of an RWG QCL, the far-field angle of a QCL with a porous region was improved by more than 70°. We computed the effective refractive index and the near-field modes using the finite element method and obtained the far-field distribution by a Fourier transformation of the simulated near field. The measurement result is very consistent with the simulated result.

The output power emitted from the front facet of the laser was measured with a thermopile detector placed directly near the window of the cryostat. The output power is not corrected by the transmission of the optics windows (BaF_2 , the transmission efficiency is about 94% for a wavelength about 4–5 μ m) and collection efficiency of the detector. Considering the absence of any focused element, the measurement results of the output power practically reflect the optical emission of the central area, which is about $\pm 30^\circ$ around the centre line of the laser beam. Figure 4 shows the central output of both the general RWG QCL and the QCL with a porous region under the pulsed driving current (2 μ s, 5 kHz, duty cycle of 1%). The device with a porous region emitted a higher peak power (267 mW)

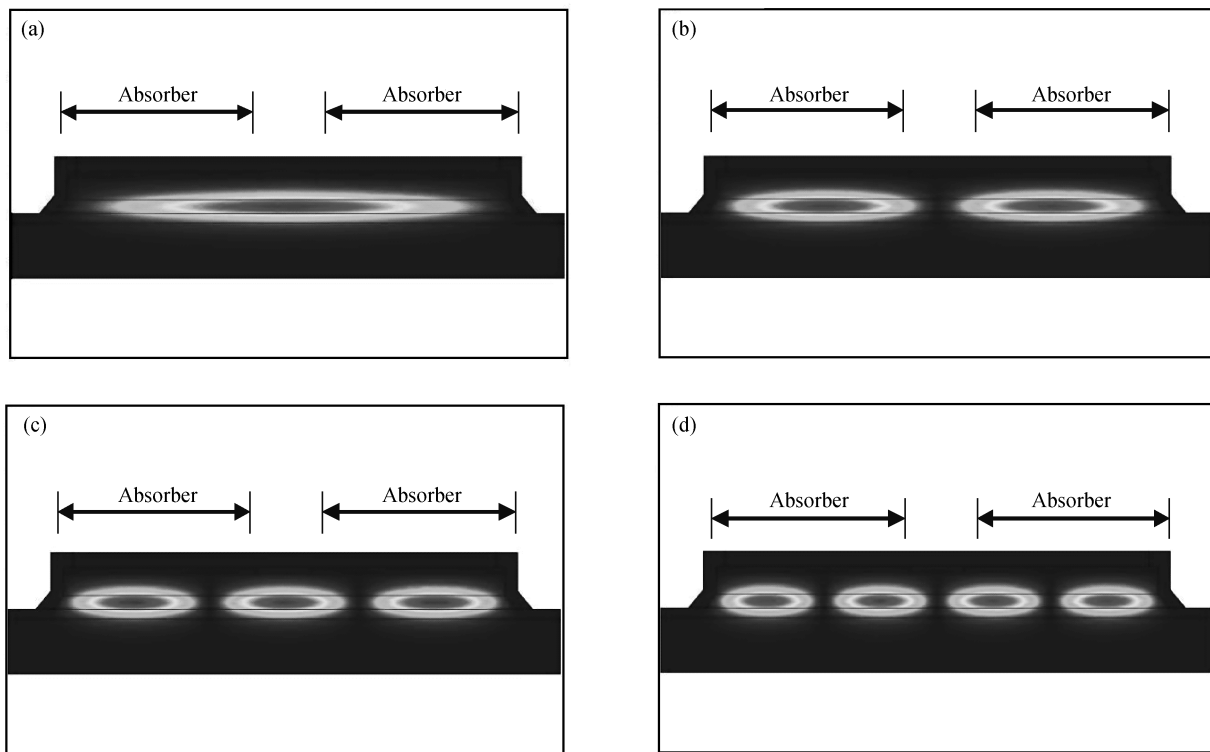


Fig. 5. Simulated near-field transverse mode imaging of a 48- μm -wide RWG QCL with side absorbers. (a) TM_{00} mode. (b) TM_{01} mode. (c) TM_{02} mode. (d) TM_{03} mode.

Table 1. Calculated waveguide loss, mirror loss, and the figure of merit of different types of devices and different transverse modes.

Type of devices	Transverse mode	Mirror loss, α_m (cm^{-1})	Waveguide loss, α_w (cm^{-1})	Figure of merit, $(\alpha_m + \alpha_w)/\Gamma$ (cm^{-1})
RWG	TM_{00}	3.6574	9.9702	20.0140
	TM_{01}	3.6190	9.9739	19.9631
	TM_{02}	3.5565	9.9787	19.8784
	TM_{03}	3.4657	9.9853	19.7576
	TM_{04}	3.3646	9.9622	19.5752
RWG with porous absorbers	TM_{00}	3.6449	15.0431	27.2978
	TM_{01}	3.6067	16.5382	29.3872
	TM_{02}	3.5422	15.2054	27.3648
	TM_{03}	3.4516	16.3470	28.8989
	TM_{04}	3.3328	15.4349	27.3981

than the general RWG QCL (34 mW) in the centre area because the general one provides more defocused laser beam. Combined with the far-field distribution result, it is clear that the RWG QCL with a porous region can meet the requirements of the practical application for its better beam quality than general RWG ones.

4. Discussion

The microporous structure fabricated by electrochemical etching, which has a branch-like morphology, can be filled by metal material (Ti/Au) during the following upper electrode growing process. This mixed structure of highly doped InP and metal on both sides of a normal ridge waveguide can be considered as porous absorbers, which provide additional absorption of optical feedback. Figure 5 shows the simulated near-field optical mode distribution of a 48- μm -wide RWG QCL

with porous absorbers. It is clear that the porous absorbers have more overlapped volume with high-order mode emission and consequently provide more absorption. As a result, the emitting of high-order transverse modes can be inhibited by this additional absorption.

In order to confirm the above opinion, the losses and threshold of both an ordinary device and a device with porous absorbers can be estimated. Simulated results based on the assumption of 10% metal material (Au) in the porous waveguide are shown in Table 1. The threshold is proportional to the figure of merit defined by $(\alpha_w + \alpha_m)/\Gamma$ ^[10]. The simulated results prove that porous absorbers greatly increase the waveguide loss of high-order modes, thereby increasing the total loss and threshold of high-order mode emission. As a result, the RWG devices with porous absorbers tend to preserve fundamental transverse mode emission, which has the lowest total loss and threshold. The calculated result is in good agreement

with the measured value.

5. Conclusion

By incorporating metal-filled porous absorber to both sides of common ridge waveguide QCL devices, we are able to switch the high-order mode to the fundamental mode and get a very small far-field divergence angle of 4.9° . This simple and low-cost fabrication process to realize high beam quality will be very useful in many applications.

References

- [1] Faist J, Capasso F, Sivco D L, et al. Quantum cascade lasers. *Science*, 1994, 264: 553
- [2] Kosterev A, Wysocki G., Bakhirkin Y, et al. Application of quantum cascade lasers to trace gas analysis. *Appl Phys B*, 2008, 90: 165
- [3] Pushkarsky M B, Dunayevskiy I G, Prasanna M, et al. High-sensitivity detection of TNT. *PNAS*, 2006, 103: 19360
- [4] Lu Q Y, Guo W H, Zhang W, et al. Room temperature operation of photonic-crystal distributed-feedback quantum cascade lasers with single longitudinal and lateral mode performance. *Appl Phys Lett*, 2010, 96: 051112
- [5] Lu Q Y, Zhang W, Wang L J, et al. Holographic fabricated photonic-crystal distributed-feedback quantum cascade laser with near-diffraction-limited beam quality. *Opt Express*, 2009, 17: 18900
- [6] Vurgaftman I, Bewley W W, Bartolo R E, et al. Far-field characteristics of mid-infrared angled-grating distributed feedback lasers. *J Appl Phys*, 2000, 88: 6997
- [7] Fan J, Belkin M A, Capasso F. Wide-ridge metal-metal terahertz quantum cascade lasers with high-order lateral mode suppression. *Appl Phys Lett*, 2008, 92: 031106
- [8] Santinacci L, Djenizian T. Electrochemical pore formation onto semiconductor surfaces. *C R Chimie*, 2008, 11: 964
- [9] Evans A, Darvish S R, Slivken J, et al. Buried heterostructure quantum cascade lasers with high continuous-wave wall plug efficiency. *Appl Phys Lett*, 2007, 91: 071107
- [10] Yu N F, Diehl L, Cubukcu E, et al. Near-field imaging of quantum cascade laser transverse modes. *Opt Express*, 2007, 15: 13227